

DiG: Differential Grounding for Enhancing Fine-Grained Perception in Multimodal Large Language Models

Zhou Tao^{1,2*}, Shida Wang^{1,2*}, Yongxiang Hua^{1,2}, Haoyu Cao^{1,2}, Linli Xu^{1,2†}

¹University of Science and Technology of China

²State Key Laboratory of Cognitive Intelligence

{zhoutao24, wangshida, yx15333063290, caohaoyu}@mail.ustc.edu.cn

linlixu@ustc.edu.cn

Abstract

Multimodal Large Language Models have achieved impressive performance on a variety of vision-language tasks, yet their fine-grained visual perception and precise spatial reasoning remain limited. In this work, we introduce DiG (Differential Grounding), a novel proxy task framework where MLLMs learn fine-grained perception by identifying and localizing all differences between similar image pairs without prior knowledge of their number. To support scalable training, we develop an automated 3D rendering-based data generation pipeline that produces high-quality paired images with fully controllable discrepancies. To address the sparsity of difference signals, we further employ curriculum learning that progressively increases complexity from single to multiple differences, enabling stable optimization. Extensive experiments demonstrate that DiG significantly improves model performance across a variety of visual perception benchmarks and that the learned fine-grained perception skills transfer effectively to standard downstream tasks, including RefCOCO, RefCOCO+, RefCOCOg, and general multimodal perception benchmarks. Our results highlight differential grounding as a scalable and robust approach for advancing fine-grained visual reasoning in MLLMs.

1. Introduction

Multimodal Large Language Models (MLLMs) have achieved remarkable progress across diverse vision-language tasks, including image captioning and visual question answering [1, 2, 5, 8, 14, 36]. While these models excel at holistic scene understanding, effectively associating global visual semantics with textual reasoning, they struggle with fine-grained visual perception and precise spatial

* Equal contribution. † Corresponding author.

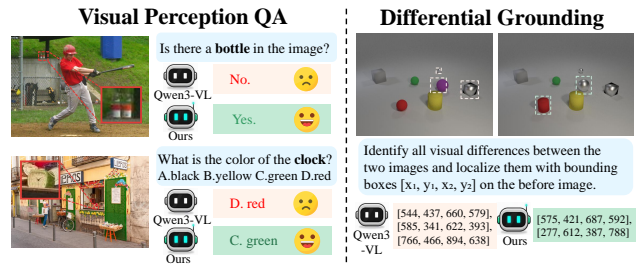


Figure 1. Illustration of Differential Grounding (DiG). **Left**: existing MLLMs fail to perceive subtle visual cues such as small object changes or color variations. **Right**: our proposed DiG task trains models to identify and localize differences between paired images, fostering fine-grained visual perception.

reasoning. As illustrated in Figure 1 (left), even state-of-the-art MLLMs often overlook subtle visual cues such as small object changes, color variations, or missing elements that are essential for detailed visual understanding. This highlights a fundamental limitation of current pretraining paradigms: while they enable strong high-level semantic alignment, they provide insufficient supervision for developing the fine-grained perceptual sensitivity required for nuanced scene analysis.

Reinforcement Learning (RL) [26, 27] has recently emerged as a powerful paradigm for enhancing the multimodal capabilities of large models. Beyond conventional supervised training, RL-based post-training has proven effective in improving robustness, alignment, and perceptual fidelity, and is now widely adopted for refining MLLMs [13, 25, 31, 45]. Building on this progress, recent studies have explored leveraging RL to strengthen visual perception in multimodal models. However, existing approaches often involve trade-offs between task specificity and generalization, or rely on costly, manually annotated datasets that limit scalability and diversity. One line of work fine-tunes models directly on traditional perceptual tasks, such as vi-

sual grounding [42]. While this approach can boost task-specific accuracy, it often produces overspecialized models that generalize poorly to open-ended multimodal understanding. Moreover, grounding datasets such as RefCOCO [16] require extensive manual annotation, making large-scale training costly and limited in diversity. Another line of research explores alternative proxy tasks, such as visual jigsaw puzzles [38, 40, 44] or caption hallucination detection [37]. Although these tasks provide useful auxiliary supervision, they are not explicitly designed to strengthen fine-grained visual perception, leaving MLLMs insufficiently sensitive to subtle visual details.

To address these limitations, we propose **DiG** (Differential Grounding), a proxy framework designed to enhance fine-grained visual perception in MLLMs through a differential image grounding task. Given two closely related images, the model is required to identify and localize all visual discrepancies without being informed of their exact number. This formulation compels the model to move beyond coarse semantic alignment and develop fine-grained perceptual reasoning. To enable scalable training, we introduce a fully automated data generation pipeline based on 3D rendering [15]. This pipeline allows precise control over the task difficulty by varying the number, subtlety, location, and type of visual differences, while ensuring accurate ground-truth annotations. As a result, it enables the construction of large-scale, high-quality datasets that provide a strong foundation for improving the perceptual capabilities of MLLMs.

A key challenge in training MLLMs on the DiG task is the extreme sparsity of difference signals: at initialization, the model rarely localizes any differences correctly, causing RL rewards to collapse near zero and preventing stable optimization. To address this, we employ a Curriculum Learning [3] (CL) strategy, progressively increasing task difficulty from simpler instances with a single discrepancy to more complex cases with multiple discrepancies. This staged approach enables stable convergence by building perceptual skills from simple to complex cases, allowing models to develop fine-grained spatial reasoning without being overwhelmed by sparse supervision.

We evaluate the effectiveness of DiG through extensive experiments. Our approach consistently improves model performance on a range of visual perception benchmarks. More importantly, the fine-grained visual perception skills acquired through DiG transfer effectively to standard downstream tasks, including fine-grained grounding benchmarks such as RefCOCO, RefCOCO+, and RefCOCOg [16], as well as general multimodal perception benchmarks [11, 20, 21, 33–35, 39]. These results demonstrate the potential of differential grounding as a scalable and robust proxy task for developing fine-grained perceptual capabilities in MLLMs. Our main contributions are:

- We introduce DiG (Differential Grounding), a novel

proxy task framework that enhances fine-grained spatial perception in MLLMs, and develop a scalable, automated data generation pipeline that produces high-quality paired images with fully controllable discrepancies.

- We propose a Curriculum Learning strategy that addresses the optimization challenges posed by the sparsity of difference signals, enabling stable and effective training on the DiG task.
- We demonstrate through extensive experiments that models trained with DiG achieve significant improvements on a range of visual perception benchmarks and exhibit strong transferability to standard fine-grained grounding datasets as well as general multimodal perception benchmarks.

2. Related Work

Reinforcement Learning for MLLMs. Reinforcement learning (RL) [19, 26, 27] has emerged as a powerful paradigm for enhancing the capabilities of multimodal large language models. With the success of rule-based RL [12, 28, 32], recent multimodal work explores RL with verifiable rewards, typically following a pipeline that conducts optional SFT activation then applies RL, such as GRPO [28], with fine-grained training recipes. Building on these advances, the MLLM community has begun extending this paradigm to enhance both visual perception and reasoning. This has spurred efforts in both dataset curation and method development. On the data front, Vision-R1 [13] and MM-Eureka [25] introduced large-scale SFT and RL datasets to facilitate effective cold-start training. Methodologically, ReasonRFT [31] and R1-VL [45] proposed novel rule-based reward functions to improve geometric understanding and spatial reasoning. Furthering this direction, Perception-R1 [42] incorporated object-matching and IoU-based reward signals to enhance fine-grained grounding performance, marking a promising step toward perceptually-aligned reinforcement learning for MLLMs.

Generalization through Proxy-task-driven Learning.

Proxy tasks have recently emerged as an effective strategy for improving generalization and reasoning in large models, offering controllable and verifiable supervision without costly human annotation. In language domains, several studies have demonstrated that solving structured synthetic problems, such as logic puzzles or rule-based games, through reinforcement learning can foster transferable reasoning abilities [4, 9, 41]. Motivated by these successes, recent multimodal research has explored analogous ideas using visually grounded proxies, including programmatically generated puzzles [38, 40, 44] and hallucination detection tasks [37]. While these approaches provide valuable intermediate supervision, most remain limited to coarse or task-

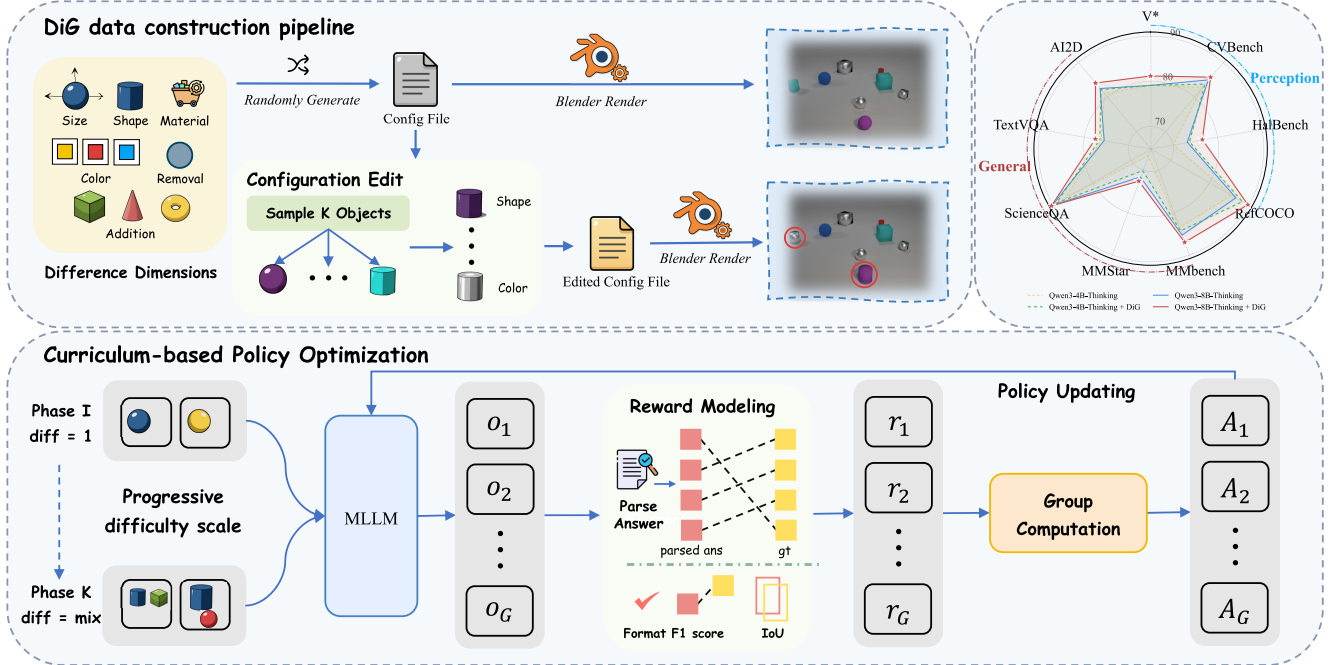


Figure 2. Overview of the proposed DiG framework. The upper part illustrates the automated 3D-based data construction pipeline that generates paired images with controllable visual differences. The lower part shows the curriculum-based policy optimization, where the MLLM is trained via GRPO with rewards for format validity, detection accuracy, and spatial precision. The radar chart on the right demonstrates consistent performance gains across both perception and general multimodal benchmarks.

specific perception. Our work extends this proxy-learning perspective to fine-grained visual understanding, formulating difference localization as a scalable, automatically verifiable grounding problem.

3. Method

Our method comprises four components. We first formalize the Differential Grounding (DiG) task, then describe a 3D-based data pipeline for generating paired images with controlled discrepancies. We further introduce a reinforcement learning objective with structured rewards and a curriculum-based training strategy to ensure stable and effective optimization.

3.1. Problem Formulation

The core of our approach is the Differential Grounding (DiG) task, which trains MLLMs to identify and localize all visual differences between image pairs. Given an input tuple $X = (I_a, I_b, P)$, where I_a denotes a reference image and I_b corresponds to its visually similar counterpart containing M subtle modifications (e.g., additions, removals, or attribute changes in objects), the model receives a textual instruction P that prompts it to identify and localize all discrepancies between the two images.

The model generates a textual output sequence $O = (o_1, o_2, \dots, o_T)$, which can be deterministically parsed into

a set of predicted bounding boxes $B_{\text{pred}} = \{b_i\}_{i=1}^N$, where each $b_i = [x_{\min}, y_{\min}, x_{\max}, y_{\max}]_i$ represents a localized discrepancy. The corresponding ground-truth annotations are given by $B_{\text{gt}} = \{b_j^{\text{gt}}\}_{j=1}^M$, which precisely mark all true differences between I_a and I_b .

The objective of DiG is to train the model such that B_{pred} aligns closely with B_{gt} in both completeness and spatial precision. Formally, this entails optimizing an objective function \mathcal{L}_{DiG} that encourages the model to perform fine-grained visual comparison, robust difference identification, and accurate spatial grounding within an open-ended generative framework.

3.2. DiG Data Construction Pipeline

To enable large-scale training for the DiG task, we construct a fully automated and scalable data generation pipeline based on the Blender 3D rendering engine. This pipeline synthesizes paired images with precisely controlled visual discrepancies and automatically produces accurate ground-truth annotations, as illustrated in Fig. 2.

The process begins with the procedural generation of a base 3D scene, where a configuration file in JSON format specifies the number of objects together with their geometric and visual attributes, including shape, material, color, size, and spatial position. This configuration file is then rendered using Blender to produce the reference image I_a .

To generate the corresponding counterpart I_b , a stochastic modification process is applied to the base configuration. An integer K is randomly sampled from the range $[1, N]$, where N denotes the maximum number of differences allowed in a scene. A total of K distinct objects are then selected, and for each object, one attribute is randomly sampled from a predefined set of modification types. This set includes changes in shape, color, size, or material, as well as object addition or removal. Applying these edits to the configuration file results in a modified version, which is subsequently rendered to obtain I_b . The resulting image pair (I_a, I_b) is visually coherent yet differs in exactly K localized regions, ensuring both realism and controllable variability across the dataset. In addition, the overall task difficulty can be flexibly extended by increasing the upper bound N , which allows the pipeline to generate more complex image pairs without altering the underlying process.

A major advantage of this rendering-based design is the ability to generate perfect ground-truth annotations automatically. Because every modification is programmatically defined in three-dimensional space, its two-dimensional projection can be extracted directly from the renderer to form the bounding-box annotations B_{gt} . This automatic supervision entirely eliminates the need for manual labeling and guarantees accurate and consistent annotations across all generated samples.

3.3. Reward Modeling and Policy Optimization

We adopt a reinforcement learning paradigm to optimize the model on the DiG task using Group Relative Policy Optimization [28] (GRPO). Given a prompt P and image pair (I_a, I_b) , the model produces a textual output O , which is parsed into predicted bounding boxes B_{pred} . The reward function consists of three complementary components that assess syntactic validity, detection accuracy, and spatial precision.

Format Reward. Since the DiG task is formulated as an open-ended generation problem, ensuring syntactic correctness is a prerequisite for any subsequent evaluation. We define a *format reward* r_{format} to encourage the model to output responses that can be deterministically parsed into valid bounding-box lists. Let $\mathcal{P}(O)$ denote a parser that extracts B_{pred} from the model’s textual output O . The reward is a binary indicator that assigns a positive signal only when the output conforms to the target schema:

$$r_{\text{format}} = \begin{cases} 1, & \text{if } \mathcal{P}(O) \neq \emptyset, \\ 0, & \text{otherwise.} \end{cases} \quad (1)$$

This component serves as a structural constraint, guiding the model to produce well-formed and machine-interpretable responses such as “[$x_{\min}, y_{\min}, x_{\max}, y_{\max}$], . . .]” rather than free-form text.

Accuracy Reward. While the format reward enforces structural correctness, it does not reflect the perceptual quality of the predicted bounding boxes. To capture the model’s fine-grained localization and detection performance, we define an *accuracy reward* r_{acc} that jointly measures the completeness and precision of detected discrepancies. Given the set of predicted boxes $B_{\text{pred}} = \{b_i\}_{i=1}^N$ and ground-truth boxes $B_{\text{gt}} = \{\tilde{b}_j\}_{j=1}^M$, we first compute a one-to-one correspondence between predictions and ground truths to ensure reliable evaluation. This is formulated as a bipartite matching problem that maximizes the overall similarity between matched pairs, solved efficiently by the Hungarian algorithm [18]. Each similarity score $\Phi(b_i, \tilde{b}_j)$ is defined as the intersection-over-union (IoU) between the two boxes, and the matched pairs \mathcal{M} are used to calculate both the detection and localization metrics.

The accuracy reward combines two complementary signals: a detection-level F1 score that reflects how completely the model identifies all differences, and an IoU term that captures the spatial alignment quality of matched boxes. Specifically, the F1 score is computed from precision $p = n_m/N$ and recall $r = n_m/M$, where n_m denotes the number of matched pairs obtained by the Hungarian assignment. The F1 score is given by $F1 = 2pr/(p+r)$, and the mean IoU is averaged over all matched pairs. The final accuracy reward is expressed as a weighted combination of these two terms:

$$r_{\text{acc}} = \lambda_1 F1 + \lambda_2 \overline{\text{IoU}} \quad (2)$$

This formulation provides a smooth and interpretable reward signal that balances holistic detection performance with precise spatial localization, and the use of bipartite matching ensures stable gradient feedback even under multiple-object discrepancies.

Overall Reward and Optimization Objective. The overall reward R integrates the structural constraint from r_{format} and the perceptual feedback from r_{acc} into a unified training signal. A small portion of the reward weight is allocated to the format term to preserve syntactic consistency while allowing the model to focus primarily on visual reasoning. The combined objective is formulated as:

$$r = (1 - \alpha)r_{\text{acc}} + \alpha r_{\text{format}}, \quad (3)$$

where α controls the relative contribution of structural validity. This hierarchical design ensures that the model first produces responses in a valid format before being rewarded for fine-grained detection and localization accuracy.

Policy Optimization. We optimize the policy π_θ using the Group Relative Policy Optimization (GRPO) [28] framework, which refines multimodal generation through group-based relative rewards. For each input (I_a, I_b, P) , the model samples G candidate responses $\{O^{(g)}\}_{g=1}^G$, each

evaluated by the reward function in Eq. (3). The normalized group-level advantage is defined as

$$A_g = \frac{r_g - \text{mean}(\{r_i\}_{i=1}^G)}{\text{std}(\{r_i\}_{i=1}^G)}, \quad (4)$$

and the token-level advantage $A_{g,t}$ is uniformly assigned to each token within $O^{(g)}$. The token-level clipped surrogate objective is formulated as

$$\mathcal{L}_{g,t}^{\text{CLIP}}(\theta) = \min(r_{g,t}A_{g,t}, \text{clip}(r_{g,t}, 1 - \varepsilon, 1 + \varepsilon)A_{g,t}), \quad (5)$$

where $r_{g,t} = \frac{\pi_{\theta}(o_t^{(g)} | o_{<t}^{(g)}, I_a, I_b, P)}{\pi_{\text{old}}(o_t^{(g)} | o_{<t}^{(g)}, I_a, I_b, P)}$ denotes the likelihood ratio for token t . The full GRPO loss integrates the expected clipped objective with a KL-divergence regularization term:

$$\begin{aligned} \mathcal{L}_{\text{GRPO}}(\theta) = & -\mathbb{E}_{O \sim \pi_{\theta}} \left[\frac{1}{G} \sum_{g=1}^G \frac{1}{|O^{(g)}|} \sum_{t=1}^{|O^{(g)}|} \mathcal{L}_{g,t}^{\text{CLIP}}(\theta) \right] \\ & + \beta D_{\text{KL}}(\pi_{\theta}(\cdot | I_a, I_b, P) \| \pi_{\text{ref}}(\cdot | I_a, I_b, P)), \end{aligned} \quad (6)$$

where β controls the trade-off between policy updates and regularization. The clip operator constrains excessive updates for stability, while the KL term penalizes deviation from the reference policy. Following [28], the KL regularization can be relaxed during early training to encourage exploration.

3.4. Curriculum-based Difficulty Scheduling

Direct optimization of the DiG task under reinforcement learning is challenging due to the extreme sparsity of informative rewards. At the early training stage, when the model is unskilled at localizing subtle visual differences, the reward signal frequently collapses to near zero, leading to unstable updates and poor convergence. To address this issue, we introduce a curriculum-based difficulty scheduling strategy that progressively increases task complexity, enabling the model to acquire fine-grained perceptual capabilities in a stable and scalable manner.

The curriculum is organized into multiple training phases of increasing difficulty, as illustrated in Fig. 2. In the initial phase, the model is trained on simple instances containing a single visual difference, which provides dense and easily interpretable feedback. This stage encourages the policy to learn the basic skill of difference localization and to establish a reliable mapping between visual perturbations and corresponding bounding-box predictions. As training proceeds, the data distribution is gradually shifted toward more complex samples containing multiple differences, promoting the development of compositional reasoning and multi-object perception. Finally, the model is fine-tuned on a mixed-difference dataset, allowing it to gen-

eralize across diverse configurations and to handle arbitrary numbers and types of discrepancies. During training on mixed-difference dataset, we abstain from providing the count of discrepancies for each image pair, tasking the model with inferring this information. This design choice elevates the task’s difficulty, offering greater potential for the model’s capability enhancement.

This progressive scheduling substantially stabilizes reinforcement learning by shaping the reward landscape from sparse to dense supervision, allowing the policy to acquire fine-grained perceptual skills through gradually structured visual comparisons.

4. Experiments

4.1. Implementation Details

Training Settings. All experiments are conducted on the proposed Differential Grounding (DiG) dataset, generated using the 3D rendering pipeline described in Sec. 3.2. The training corpus comprises approximately 4.8K image pairs, split evenly across three subsets: single-difference, double-difference, and mixed-difference (about 1.6K each). Mixed-difference scenes contain up to four visual discrepancies. We adopt Qwen3-VL-8B-Thinking and Qwen3-VL-4B-Thinking [2] as multimodal backbones, and perform reinforcement post-training using the verl [29] framework with the GRPO objective and KL-regularized policy optimization. Training follows the curriculum strategy detailed in Sec. 3.4, gradually increasing task complexity from simple to mixed-difference instances. All implementation and hyperparameter details are provided in the Appendix.

Evaluation Setup. We evaluate the proposed approach on a comprehensive suite of multimodal benchmarks covering visual perception, grounding, and general understanding. The perception evaluation includes HalBench [11], HRBench-8K [35], POPE [20], V* [39], VSR [21], CV-Bench [33], and MMVP [34]. Grounding performance is assessed on RefCOCO, RefCOCO+, and RefCOCOg [16], while broader multimodal reasoning and comprehension are examined on MMBench [23], MM-Vet [43], MM-Star [6], ScienceQA [24], TextVQA [30], MME [10], and AI2D [17]. All evaluations follow the standard protocols of each benchmark to ensure fairness and reproducibility, with detailed settings provided in the Appendix.

4.2. Main Results

Performance on Perception Benchmarks. As shown in Tab. 1, DiG consistently improves both the 4B and 8B variants of Qwen3-VL-Thinking across a broad range of perception-oriented benchmarks. Notably, the 8B model achieves substantial gains of +3.4 on HalBench and +2.1 on V*, accompanied by steady improvements on VSR and

Table 1. **Performance on perception benchmarks.** Comparison across various multimodal perception benchmarks including HalBench, HRB8K, POPE, V*, VSR, CV-Bench, and MMVP. Integrating DiG consistently improves fine-grained perception and spatial reasoning for both Qwen3-VL-4B and Qwen3-VL-8B models over their respective base counterparts.

Model	HalBench	HRB8K	POPE	V*	VSR	CV-Bench	MMVP	AVG
Qwen2.5-VL-7B [2]	50.1	65.3	86.4	77.0	77.7	64.9	54.7	68.0
Qwen2.5-VL-72B [2]	55.2	77.1	–	85.9	–	83.0	81.7	–
InternVL2.5-78B [7]	57.1	72.5	90.8	75.9	–	–	83.0	–
Qwen3-VL-4B-Thinking	70.1	69.3	88.3	79.1	82.5	82.8	80.0	78.9
+ DiG (Ours)	73.8 ^{+3.8}	71.0 ^{+1.7}	88.5 ^{+0.2}	79.1	83.9 ^{+1.4}	83.8 ^{+1.0}	79.0 ^{+1.0}	79.9 ^{+1.0}
Qwen3-VL-8B-Thinking	73.3	69.9	87.9	79.1	82.6	85.0	77.3	79.3
+ DiG (Ours)	76.7 ^{+3.4}	70.4 ^{+0.5}	88.0 ^{+0.1}	81.2 ^{+2.1}	83.0 ^{+0.4}	85.8 ^{+0.8}	78.7 ^{+1.4}	80.5 ^{+1.2}

Table 2. **Performance on general multimodal benchmarks.** Evaluation on standard multimodal benchmarks including MMBench, MMVet, MMStar, SQA^I, VQA^T, MME, and A12D. Incorporating DiG into Qwen3-VL models consistently enhances overall reasoning and perception capabilities, demonstrating strong transferability beyond fine-grained tasks.

Model	LLM	MMBench	MMVet	MMStar	SQA ^I	VQA ^T	MME	A12D
LLaVA-NeXT [22]	Vicuna1.5-7B	67.4	43.9	37.7	70.1	64.9	1519	66.6
InternVL3.5-38B [36]	Qwen3-32B	87.3	82.2	75.3	–	82.7	–	87.8
Qwen2.5-VL 72B [2]	Qwen2.5-72B	88.6	76.2	70.8	–	84.9	–	83.9
Qwen3-VL	Qwen3-4B	83.7	76.0	66.7	86.9	76.2	1592.4	81.0
+ DiG (Ours)	Qwen3-4B	84.5 ^{+0.8}	77.3 ^{+1.3}	70.2 ^{+3.5}	89.2 ^{+2.3}	76.5 ^{+0.3}	1643.4 ^{+51.0}	82.2 ^{+1.2}
Qwen3-VL	Qwen3-8B	85.5	76.4	71.7	90.3	75.5	1648.4	82.5
+ DiG (Ours)	Qwen3-8B	87.2 ^{+2.2}	76.8 ^{+0.4}	72.7 ^{+1.0}	90.5 ^{+0.2}	77.5 ^{+2.0}	1665.9 ^{+17.5}	84.1 ^{+1.6}

CV-Bench. The 4B variant follows a similar trend, yielding up to +3.8 improvement on HalBench and noticeable gains on HRB8K and VSR, confirming that the proposed differential grounding generalizes effectively across different model scales. These consistent enhancements indicate that DiG strengthens the model’s sensitivity to fine-grained visual cues and its ability to maintain spatial consistency under complex visual perturbations, leading to reduced hallucination and enhanced perceptual fidelity. Taken together, these results highlight that differential grounding provides a scalable and principled way to reinforce fine-grained perceptual understanding and bridge structured perception with higher-level multimodal reasoning.

Performance on General Multimodal Benchmarks.

We further evaluate DiG on a suite of comprehensive multimodal benchmarks that jointly assess holistic perception and reasoning ability, as summarized in Tab. 2. Across all evaluated tasks, DiG delivers consistent performance gains for both the 4B and 8B variants of Qwen3-VL, demonstrating the generality and robustness of the proposed reinforcement formulation. The 4B model achieves notable improvements of +3.5 on MMStar and +2.3 on ScienceQA, while the 8B model exhibits steady gains on MMBench (+2.2) and MME (+17.5), indicating that differential grounding effectively strengthens multimodal reasoning

and structured visual-text alignment. Such enhancements are particularly remarkable given that DiG-equipped models, despite their relatively smaller scale, achieve performance comparable to or exceeding that of several larger proprietary systems reported in prior literature. This suggests that the improvements brought by DiG stem from more efficient representation learning and better reward-driven perception refinement rather than model size alone. Overall, these results confirm that DiG fosters more structured multimodal understanding, enabling models to better integrate visual perception with abstract reasoning under a unified reinforcement framework.

Performance on Grounding Benchmarks.

Tab. 3 summarizes the results on the RefCOCO, RefCOCO+, and RefCOCOG benchmarks, which evaluate fine-grained visual grounding under varying linguistic and spatial conditions. Across all datasets and evaluation splits, models trained with DiG consistently outperform their base counterparts, demonstrating the effectiveness of differential grounding in improving region-level perception. Specifically, the 8B variant achieves average improvements of approximately 2–3 points across all benchmarks, with particularly strong gains on RefCOCO (+2.0–+3.4) and RefCOCO+ (+2.0–+3.0), while the 4B model exhibits comparable trends. These results indicate that DiG substantially enhances spa-

Table 3. Evaluation on visual grounding benchmarks. Results on referring expression comprehension datasets RefCOCO, RefCOCO+, and RefCOCOg. Incorporating DiG into Qwen3-VL models consistently improves localization accuracy across different IoU thresholds, demonstrating stronger fine-grained spatial grounding and generalization ability. The expert model is denoted in gray.

RefCOCO													
method	size	val@50	testA@50	testB@50	val@75	testA@75	testB@75	val@95	testA@95	testB@95	val _{avg}	testA _{avg}	testB _{avg}
Qwen3-VL	4B	85.7	90.1	79.1	77.6	81.9	69.0	28.7	30.8	23.1	64.0	67.6	57.1
+ DiG (Ours)	4B	88.6	91.5	83.5	80.3	83.5	72.3	31.6	35.2	26.6	66.8	70.1	60.8
Qwen3-VL	8B	86.9	90.6	81.7	78.9	82.5	70.9	29.1	31.3	23.8	65.0	68.1	58.8
+ DiG (Ours)	8B	90.0	91.9	86.4	81.0	84.0	74.9	29.9	33.9	25.3	67.0	69.9	62.2

RefCOCO+													
method	size	val@50	testA@50	testB@50	val@75	testA@75	testB@75	val@95	testA@95	testB@95	val _{avg}	testA _{avg}	testB _{avg}
Qwen3-VL	4B	80.3	87.0	72.9	72.8	78.8	63.6	27.0	29.6	21.7	60.0	65.1	52.7
+ DiG (Ours)	4B	82.9	87.4	76.4	75.2	79.3	66.3	29.9	33.8	24.3	62.6	66.8	55.7
Qwen3-VL	8B	81.8	86.6	73.9	74.0	78.5	64.6	27.9	30.9	21.7	61.2	65.3	53.4
+ DiG (Ours)	8B	84.2	87.7	77.6	76.1	80.1	68.1	28.6	32.2	23.5	63.0	66.7	56.4

RefCOCOg										
method	size	val@50	test@50	val@75	test@75	val@95	test@95	val _{avg}	test _{avg}	
Qwen3-VL	4B	85.0	85.0	75.2	76.1	27.1	27.6	62.4	62.9	
+ DiG (Ours)	4B	87.2	87.2	77.8	78.2	30.7	31.2	65.3	65.6	
Qwen3-VL	8B	86.3	86.5	76.1	77.0	26.3	27.4	62.9	63.6	
+ DiG (Ours)	8B	87.7	88.0	77.7	78.5	28.8	29.8	64.7	65.4	

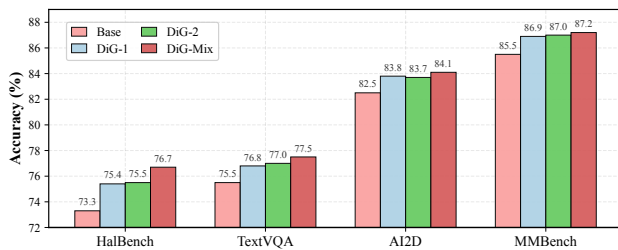


Figure 3. Ablation on curriculum scheduling in DiG training. Progressively increasing task complexity from single-difference (DiG-1) to double-difference (DiG-2) and mixed-difference (DiG-Mix) leads to consistent performance gains across HalBench, TextVQA, AI2D, and MMBench.

tial reasoning and fine-grained localization, enabling more accurate alignment between referring expressions and visual regions. We attribute this improvement not only to the reinforcement of object-level perceptual precision, but also to the grounding-oriented output format adopted during optimization, which provides consistent supervision and stabilizes multimodal alignment during policy refinement.

4.3. Ablation Study and Analysis

Ablation on Curriculum Scheduling. To evaluate the effectiveness of the proposed curriculum-based optimization, we conduct an ablation study across different stages of the DiG training pipeline. As shown in Fig. 3, the

Table 4. Ablation on reward components. Evaluating different reward terms in DiG shows that combining spatial (IoU) and detection (F1) signals yields the best overall performance across RefCOCO, HalBench, MMBench, and AI2D.

Format	IoU	F1	RefCOCO			HalBench	MMB	AI2D
			val@50	testA@50	testB@50			
✓	✗	✗	-	-	-	-	-	
✓	✓	✗	84.2	89.3	76.7	70.8	83.2	81.7
✓	✗	✓	87.8	91.1	82.4	72.8	84.4	82.1
✓	✓	✓	88.6	91.5	83.5	73.8	84.5	82.2

model trained on the single-difference stage (DiG-1) already achieves clear gains over the base model, indicating that fine-grained discrepancy supervision effectively enhances perceptual alignment. Building upon DiG-1, further training on the double-difference stage (DiG-2) yields additional gains on most benchmarks, indicating the benefit of progressively increasing perceptual complexity. Finally, fine-tuning on the mixed-difficulty data (DiG-Mix) leads to the best overall performance, confirming that progressive exposure to increasingly complex visual discrepancies yields more robust and generalizable visual understanding.

Ablation on Reward. We further analyze the effect of different reward components by selectively activating the IoU and F1 terms while keeping the format reward enabled (Tab. 4). Relying solely on IoU leads to a noticeable perfor-

mance drop, suggesting that spatial overlap alone does not sufficiently capture task success, as the model can obtain relatively high IoU scores without correctly identifying all target regions. In contrast, using only the F1-based reward improves precision by emphasizing detection completeness but still lacks stable spatial grounding. Integrating both IoU and F1 yields the best overall performance, achieving 88.6/91.5/83.5 on RefCOCO and consistent gains across HalBench, MMBench, and AI2D. These findings demonstrate that a balanced combination of spatial and categorical signals is essential for shaping an informative reward landscape and guiding the model toward holistic grounding behavior.

Case Study on Differential Grounding Dynamics. To better understand the learning behavior of our model, we visualize its intermediate predictions during reinforcement optimization on a validation sample, as shown in Fig. 4. The model progressively refines its localization of visual discrepancies, evolving from coarse and partially incorrect bounding boxes at early steps to precise and consistent detections after convergence. This gradual improvement reflects the emergence of fine-grained perceptual alignment between the reference and modified images, indicating that the model gradually internalizes the notion of differential grounding through reinforcement feedback.

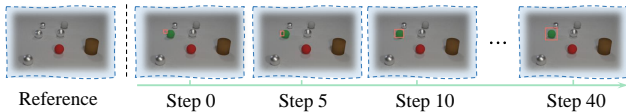


Figure 4. Visualization of differential grounding dynamics. The model progressively refines discrepancy localization from coarse initial predictions to precise detections, revealing the emergence of fine-grained perceptual alignment during reinforcement learning.

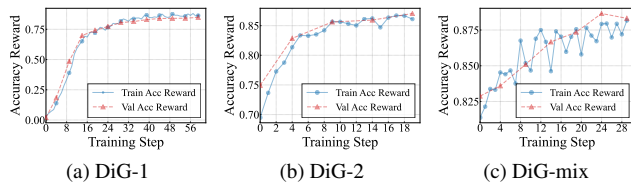


Figure 5. Accuracy reward across curriculum stages of DiG.

Curriculum Optimization Behavior. We visualize the accuracy reward during reinforcement learning across the three curriculum stages in Fig. 5. As shown in the figure, the model initially struggles to obtain meaningful rewards, reflecting the difficulty of optimizing fine-grained perception from sparse feedback. In the single-difference stage (DiG-1), the reward rises rapidly as the model learns to detect and localize basic visual discrepancies. Subsequent training on

the double-difference stage (DiG-2) further refines spatial reasoning and stabilizes convergence. Finally, the mixed-difficulty stage (DiG-Mix) maintains steady improvements under increased task complexity, indicating that curriculum scheduling effectively mitigates reward sparsity and facilitates robust policy optimization.

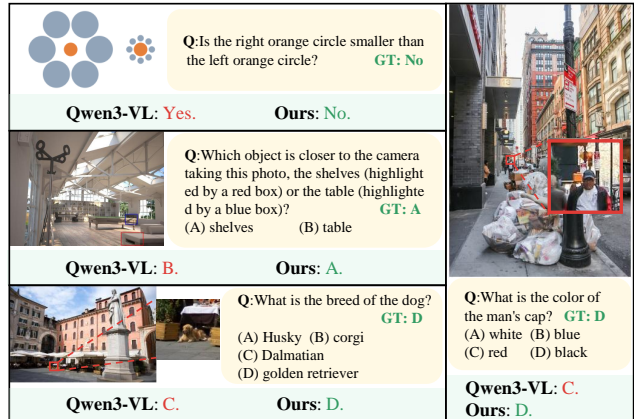


Figure 6. Case study on fine-grained visual reasoning. Our model yields more accurate responses than Qwen3-VL, particularly for subtle spatial and attribute-based questions.

Qualitative Analysis. We further present qualitative examples in Fig. 6 to illustrate the effect of DiG on fine-grained visual reasoning. Compared with the baseline Qwen3-VL, our model produces more accurate answers for queries involving subtle spatial relations and object-level attributes. In the first two cases, the baseline fails to correctly judge relative size and depth ordering, while our model provides consistent and spatially coherent predictions. Similarly, in the lower examples, our model accurately recognizes fine attribute details such as color and object category that are easily overlooked by the baseline. These results highlight that DiG enhances the model’s sensitivity to local visual discrepancies and strengthens its capacity for precise perceptual reasoning beyond coarse semantic understanding.

5. Conclusion

In this work, we introduced DiG (Differential Grounding), a novel proxy framework designed to enhance fine-grained visual perception and spatial reasoning in multimodal large language models. By framing differential comparison between paired images as a grounding task, DiG encourages models to develop precise visual discrimination and object-level awareness beyond conventional semantic alignment. Our automated 3D rendering pipeline enables scalable data synthesis with controllable discrepancies, while the curriculum-based reinforcement learning strategy effectively mitigates reward sparsity and stabilizes optimization. Extensive experiments across perception, grounding, and

general benchmarks demonstrate that DiG consistently improves fine-grained perceptual capability and generalization across scales. We believe that differential grounding offers a scalable and principled paradigm for bridging high-level reasoning and low-level perception in multimodal large language models, and provides a promising direction toward more perceptually aligned multimodal intelligence.

References

- [1] Jinze Bai, Shuai Bai, Yunfei Chu, Zeyu Cui, Kai Dang, Xiaodong Deng, Yang Fan, Wenbin Ge, Yu Han, Fei Huang, et al. Qwen technical report. *arXiv preprint arXiv:2309.16609*, 2023. 1
- [2] Shuai Bai, Keqin Chen, Xuejing Liu, Jialin Wang, Wenbin Ge, Sibao Song, Kai Dang, Peng Wang, Shijie Wang, Jun Tang, et al. Qwen2. 5-vl technical report. *arXiv preprint arXiv:2502.13923*, 2025. 1, 5, 6
- [3] Yoshua Bengio, Jérôme Louradour, Ronan Collobert, and Jason Weston. Curriculum learning. In *Proceedings of the 26th annual international conference on machine learning*, pages 41–48, 2009. 2
- [4] Jiangjie Chen, Qianyu He, Siyu Yuan, Aili Chen, Zhicheng Cai, Weinan Dai, Hongli Yu, Qiyang Yu, Xuefeng Li, Jiaye Chen, et al. Enigmata: Scaling logical reasoning in large language models with synthetic verifiable puzzles. *arXiv preprint arXiv:2505.19914*, 2025. 2
- [5] Lin Chen, Jinsong Li, Xiaoyi Dong, Pan Zhang, Conghui He, Jiaqi Wang, Feng Zhao, and Dahua Lin. Sharegpt4v: Improving large multi-modal models with better captions. In *European Conference on Computer Vision*, pages 370–387. Springer, 2024. 1
- [6] Lin Chen, Jinsong Li, Xiaoyi Dong, Pan Zhang, Yuhang Zang, Zehui Chen, Haodong Duan, Jiaqi Wang, Yu Qiao, Dahua Lin, et al. Are we on the right way for evaluating large vision-language models? *Advances in Neural Information Processing Systems*, 37:27056–27087, 2024. 5
- [7] Zhe Chen, Weiyun Wang, Yue Cao, Yangzhou Liu, Zhangwei Gao, Erfei Cui, Jinguo Zhu, Shenglong Ye, Hao Tian, Zhaoyang Liu, et al. Expanding performance boundaries of open-source multimodal models with model, data, and test-time scaling, 2025. URL <https://arxiv.org/abs/2412.05271>, 2025. 6
- [8] Gheorghe Comanici, Eric Bieber, Mike Schaekermann, Ice Pasupat, Naveen Sachdeva, Inderjit Dhillon, Marcel Blisstein, Ori Ram, Dan Zhang, Evan Rosen, et al. Gemini 2.5: Pushing the frontier with advanced reasoning, multimodality, long context, and next generation agentic capabilities. *arXiv preprint arXiv:2507.06261*, 2025. 1
- [9] Qingxiu Dong, Li Dong, Yao Tang, Tianzhu Ye, Yutao Sun, Zhifang Sui, and Furu Wei. Reinforcement pre-training. *arXiv preprint arXiv:2506.08007*, 2025. 2
- [10] Chaoyou Fu, Peixian Chen, Yunhang Shen, Yulei Qin, Mengdan Zhang, Xu Lin, Jinrui Yang, Xiawu Zheng, Ke Li, Xing Sun, et al. Mme: A comprehensive evaluation benchmark for multimodal large language models. *arXiv preprint arXiv:2306.13394*, 2023. 5
- [11] Tianrui Guan, Fuxiao Liu, Xiyang Wu, Ruiqi Xian, Zongxia Li, Xiaoyu Liu, Xijun Wang, Lichang Chen, Furong Huang, Yaser Yacoob, et al. Hallusionbench: an advanced diagnostic suite for entangled language hallucination and visual illusion in large vision-language models. In *Proceedings of the IEEE/CVF Conference on Computer Vision and Pattern Recognition*, pages 14375–14385, 2024. 2, 5
- [12] Daya Guo, Dejian Yang, Haowei Zhang, Junxiao Song, Peiyi Wang, Qihao Zhu, Runxin Xu, Ruoyu Zhang, Shirong Ma, Xiao Bi, et al. Deepseek-r1 incentivizes reasoning in llms through reinforcement learning. *Nature*, 645(8081):633–638, 2025. 2
- [13] Wenxuan Huang, Bohan Jia, Zijie Zhai, Shaosheng Cao, Zheyu Ye, Fei Zhao, Zhe Xu, Yao Hu, and Shaohui Lin. Vision-r1: Incentivizing reasoning capability in multimodal large language models. *arXiv preprint arXiv:2503.06749*, 2025. 1, 2
- [14] Aaron Hurst, Adam Lerer, Adam P Goucher, Adam Perelman, Aditya Ramesh, Aidan Clark, AJ Ostrow, Akila Welihinda, Alan Hayes, Alec Radford, et al. Gpt-4o system card. *arXiv preprint arXiv:2410.21276*, 2024. 1
- [15] Justin Johnson, Bharath Hariharan, Laurens Van Der Maaten, Li Fei-Fei, C Lawrence Zitnick, and Ross Girshick. Clevr: A diagnostic dataset for compositional language and elementary visual reasoning. In *Proceedings of the IEEE conference on computer vision and pattern recognition*, pages 2901–2910, 2017. 2
- [16] Sahar Kazemzadeh, Vicente Ordonez, Mark Matten, and Tamara Berg. ReferItGame: Referring to objects in photographs of natural scenes. In *Proceedings of the 2014 Conference on Empirical Methods in Natural Language Processing (EMNLP)*, pages 787–798, Doha, Qatar, 2014. Association for Computational Linguistics. 2, 5
- [17] Aniruddha Kembhavi, Mike Salvato, Eric Kolve, Minjoon Seo, Hannaneh Hajishirzi, and Ali Farhadi. A diagram is worth a dozen images. In *European conference on computer vision*, pages 235–251. Springer, 2016. 5
- [18] Harold W Kuhn. The hungarian method for the assignment problem. *Naval research logistics quarterly*, 2(1-2):83–97, 1955. 4
- [19] Nathan Lambert, Jacob Morrison, Valentina Pyatkin, Shengyi Huang, Hamish Ivison, Faeze Brahman, Lester James V Miranda, Alisa Liu, Nouha Dziri, Shane Lyu, et al. Tulu 3: Pushing frontiers in open language model post-training. *arXiv preprint arXiv:2411.15124*, 2024. 2
- [20] Yifan Li, Yifan Du, Kun Zhou, Jinpeng Wang, Wayne Xin Zhao, and Ji-Rong Wen. Evaluating object hallucination in large vision-language models. *arXiv preprint arXiv:2305.10355*, 2023. 2, 5
- [21] Fangyu Liu, Guy Emerson, and Nigel Collier. Visual spatial reasoning. *Transactions of the Association for Computational Linguistics*, 11:635–651, 2023. 2, 5
- [22] Haotian Liu, Chunyuan Li, Yuheng Li, Bo Li, Yuanhan Zhang, Sheng Shen, and Yong Jae Lee. Llava-next: Improved reasoning, ocr, and world knowledge, 2024. 6
- [23] Yuan Liu, Haodong Duan, Yuanhan Zhang, Bo Li, Songyang Zhang, Wangbo Zhao, Yike Yuan, Jiaqi Wang, Conghui He,

- Ziwei Liu, et al. Mmbench: Is your multi-modal model an all-around player? In *European conference on computer vision*, pages 216–233. Springer, 2024. 5
- [24] Pan Lu, Swaroop Mishra, Tanglin Xia, Liang Qiu, Kai-Wei Chang, Song-Chun Zhu, Oyvind Tafford, Peter Clark, and Ashwin Kalyan. Learn to explain: Multimodal reasoning via thought chains for science question answering. *Advances in Neural Information Processing Systems*, 35:2507–2521, 2022. 5
- [25] Fanqing Meng, Lingxiao Du, Zongkai Liu, Zhixiang Zhou, Quanfeng Lu, Daocheng Fu, Botian Shi, Wenhai Wang, Junjun He, Kaipeng Zhang, et al. Mm-eureka: Exploring visual aha moment with rule-based large-scale reinforcement learning. *CoRR*, 2025. 1, 2
- [26] Rafael Rafailov, Archit Sharma, Eric Mitchell, Christopher D Manning, Stefano Ermon, and Chelsea Finn. Direct preference optimization: Your language model is secretly a reward model. *Advances in neural information processing systems*, 36:53728–53741, 2023. 1, 2
- [27] John Schulman, Filip Wolski, Prafulla Dhariwal, Alec Radford, and Oleg Klimov. Proximal policy optimization algorithms. *arXiv preprint arXiv:1707.06347*, 2017. 1, 2
- [28] Zhihong Shao, Peiyi Wang, Qihao Zhu, Runxin Xu, Junxiao Song, Xiao Bi, Haowei Zhang, Mingchuan Zhang, YK Li, Yang Wu, et al. Deepseekmath: Pushing the limits of mathematical reasoning in open language models. *arXiv preprint arXiv:2402.03300*, 2024. 2, 4, 5
- [29] Guangming Sheng, Chi Zhang, Zilingfeng Ye, Xibin Wu, Wang Zhang, Ru Zhang, Yanghua Peng, Haibin Lin, and Chuan Wu. Hybridflow: A flexible and efficient rlhf framework. In *Proceedings of the Twentieth European Conference on Computer Systems*, pages 1279–1297, 2025. 5
- [30] Amanpreet Singh, Vivek Natarajan, Meet Shah, Yu Jiang, Xinlei Chen, Dhruv Batra, Devi Parikh, and Marcus Rohrbach. Towards vqa models that can read. In *Proceedings of the IEEE/CVF conference on computer vision and pattern recognition*, pages 8317–8326, 2019. 5
- [31] Huajie Tan, Yuheng Ji, Xiaoshuai Hao, Minglan Lin, Pengwei Wang, Zhongyuan Wang, and Shanghang Zhang. Reason-rlf: Reinforcement fine-tuning for visual reasoning. *arXiv preprint arXiv:2503.20752*, 2025. 1, 2
- [32] Kimi Team, Angang Du, Bofei Gao, Bawei Xing, Changjiu Jiang, C Chen, C Li, C Xiao, C Du, C Liao, et al. Kimi k1. 5: Scaling reinforcement learning with llms, 2025. URL <https://arxiv.org/abs/2501.12599>, 2025. 2
- [33] Peter Tong, Ellis Brown, Penghao Wu, Sanghyun Woo, Adithya Jairam Vedagiri IYER, Sai Charitha Akula, Shusheng Yang, Jihan Yang, Manoj Middepogu, Ziteng Wang, et al. Cambrian-1: A fully open, vision-centric exploration of multimodal llms. *Advances in Neural Information Processing Systems*, 37:87310–87356, 2024. 2, 5
- [34] Shengbang Tong, Zhuang Liu, Yuexiang Zhai, Yi Ma, Yann LeCun, and Saining Xie. Eyes wide shut? exploring the visual shortcomings of multimodal llms. In *Proceedings of the IEEE/CVF Conference on Computer Vision and Pattern Recognition*, pages 9568–9578, 2024. 5
- [35] Wenbin Wang, Liang Ding, Minyan Zeng, Xiabin Zhou, Li Shen, Yong Luo, Wei Yu, and Dacheng Tao. Divide, conquer and combine: A training-free framework for high-resolution image perception in multimodal large language models. In *Proceedings of the AAAI Conference on Artificial Intelligence*, pages 7907–7915, 2025. 2, 5
- [36] Weiyun Wang, Zhangwei Gao, Lixin Gu, Hengjun Pu, Long Cui, Xingguang Wei, Zhaoyang Liu, Linglin Jing, Shenglong Ye, Jie Shao, et al. Internvl3. 5: Advancing open-source multimodal models in versatility, reasoning, and efficiency. *arXiv preprint arXiv:2508.18265*, 2025. 1, 6
- [37] Xiyao Wang, Zhengyuan Yang, Chao Feng, Yongyuan Liang, Yuhang Zhou, Xiaoyu Liu, Ziyi Zang, Ming Li, Chung-Ching Lin, Kevin Lin, et al. Vicrit: A verifiable reinforcement learning proxy task for visual perception in vlms. *arXiv preprint arXiv:2506.10128*, 2025. 2
- [38] Zifu Wang, Junyi Zhu, Bo Tang, Zhiyu Li, Feiyu Xiong, Jiaqian Yu, and Matthew B Blaschko. Jigsaw-rl: A study of rule-based visual reinforcement learning with jigsaw puzzles. *arXiv preprint arXiv:2505.23590*, 2025. 2
- [39] Penghao Wu and Saining Xie. V?: Guided visual search as a core mechanism in multimodal llms. In *Proceedings of the IEEE/CVF Conference on Computer Vision and Pattern Recognition*, pages 13084–13094, 2024. 2, 5
- [40] Penghao Wu, Yushan Zhang, Haiwen Diao, Bo Li, Lewei Lu, and Ziwei Liu. Visual jigsaw post-training improves mllms. *arXiv preprint arXiv:2509.25190*, 2025. 2
- [41] Tian Xie, Zitian Gao, Qingnan Ren, Haoming Luo, Yuqian Hong, Bryan Dai, Joey Zhou, Kai Qiu, Zhirong Wu, and Chong Luo. Logic-rl: Unleashing llm reasoning with rule-based reinforcement learning. *arXiv preprint arXiv:2502.14768*, 2025. 2
- [42] En Yu, Kangheng Lin, Liang Zhao, Jisheng Yin, Yana Wei, Yuang Peng, Haoran Wei, Jianjian Sun, Chunrui Han, Zheng Ge, et al. Perception-rl: Pioneering perception policy with reinforcement learning. *arXiv preprint arXiv:2504.07954*, 2025. 2
- [43] Weihao Yu, Zhengyuan Yang, Linjie Li, Jianfeng Wang, Kevin Lin, Zicheng Liu, Xinchao Wang, and Lijuan Wang. Mm-vet: Evaluating large multimodal models for integrated capabilities. *arXiv preprint arXiv:2308.02490*, 2023. 5
- [44] Yu Zeng, Wenxuan Huang, Shiting Huang, Xikun Bao, Yukun Qi, Yiming Zhao, Qiuchen Wang, Lin Chen, Zehui Chen, Huaian Chen, et al. Agentic jigsaw interaction learning for enhancing visual perception and reasoning in vision-language models. *arXiv preprint arXiv:2510.01304*, 2025. 2
- [45] Jingyi Zhang, Jiaying Huang, Huanjin Yao, Shunyu Liu, Xikun Zhang, Shijian Lu, and Dacheng Tao. RL-vl: Learning to reason with multimodal large language models via step-wise group relative policy optimization. *arXiv preprint arXiv:2503.12937*, 2025. 1, 2